http://dx.doi.org/10.5012/bkcs.2013.34.8.2408

Synthesis and Characterization of Magnetic Nanoparticles and Its Application in Lipase Immobilization

Jiakun Xu,[†,‡,*] Caixia Ju,[†,§] Jun Sheng,[†] Fang Wang,[†] Quan Zhang,[†,§] Guolong Sun,[†,#] and Mi Sun[†,*]

[†]*Key Laboratory for Sustainable Utilization of Marine Fisheries Resources, Ministry of Agruculture, Yellow Sea Fisheries Research Institute, Chinese Academy of Fishery Sciences, Qingdao 266071, China*
[*]*E-mail: xujk@ysfri.ac.cn (J. Xu); hhsunmi@yeah.net (M. Sun)*
[‡]*Key Laboratory of Marine Chemistry Theory and Technology, Ministry of Education, Ocean University of China, Qingdao 266100, China*
[§]*College of Food Science and Technology, Shanghai Ocean University, Shanghai 201306, China*
[#]*College of Food Science and Engineering, Dalian Ocean University, Dalian 116023, China*
Received April 22, 2013, Accepted May 20, 2013

We demonstrate herein the synthesis and modification of magnetic nanoparticles and its use in the immobilization of the lipase. Magnetic Fe_3O_4 nanoparticles (MNPs) were prepared by simple co-precipitation method in aqueous medium and then subsequently modified with tetraethyl orthosilicate (TEOS) and 3-aminopropyl triethylenesilane (APTES). Silanization magnetic nanoparticles (SMNP) and amino magnetic nanomicrosphere (AMNP) were synthesized successfully. The morphology, structure, magnetic property and chemical composition of the synthetic MNP and its derivatives were characterized using transmission electron microscopy (TEM), Fourier transform infrared spectroscopy (FT-IR) analysis, X-ray diffraction, superconducting quantum interference device (SQUID) and thermogravimetric analyses (TGA). All of these three nanoparticles exhibited good crystallization performance, apparent superparamagnetism, and the saturation magnetization of MNP, SMNP, AMNP were 47.9 emu/g, 33.0 emu/g and 19.5 emu/g, respectively. The amino content was 5.66%. The AMNP was used to immobilize lipase, and the maximum adsorption capacity of the protein was 26.3 mg/g. The maximum maintained activity (88 percent) was achieved while the amount of immobilized lipase was 23.7 mg g^{-1}. Immobilization of enzyme on the magnetic nanoparticles can facilitate the isolation of reaction products from reaction mixture and thus lowers the cost of enzyme application.

Key Words : Magnetic nanoparticle, Surface modification, Lipase, Protein immobilization

Introduction

Much efforts have been devoted to the research on metal oxide nanoparticles due to their properties such as superparamagnetism, high surface area, large surface-to-volume ratio, easy separation under external magnetic fields.[1-3] From the past few decades, nanosized iron oxide particles have attracted great attention in the fields including, but not limited to, immunoassay,[4,5] biosensor,[6,7] bioseparation,[8,9] targeted drug delivery,[10,11] and environmental analysis[12,13] and protein immobilization.[14-21] However, the bare Fe_3O_4 NPs have high reactivity and easily undergo degradation upon direct exposing to certain environment, leading to poor stability and dispersity. Therefore, the surface of magnetic nanoparticles should be modified to improve the dispersity and biocompatibility, which could significantly facilitate its utilization.

From more than 500 strains of marine microorganisms, we isolated a marine yeast Bohaisea-9145, which can secrete marine cold-adapted lipase with good properties such as high catalytic activity at low-temperature, good stability under alkaline conditions, good compatibility with metal ions and high affinity to a number of long-chain substrates.[22-24] Therefore, the enzyme has good application prospects. However, the application of free lipase-catalyzed reactions in industrial production encounters various limitations such as two-phase separation difficulty, difficult recovery and easy aggregation in the course of the reaction. Immobilized enzyme technology can overcome these shortcomings of the free enzyme, which could lower the cost of enzyme applications and further broaden their industrial applications.[25-27]

In this work, monodisperse Fe_3O_4 NPs were initially synthesized using coprecipiation method, and subsequently coated with silica to form a outer silica shell, then the surface modification of these particles through the grafting of aminopropylsilane groups (3-aminopropyl) triethoxysilane (APTES). The as-synthesized magnetic NPs were utilized for lipase immobilization, which could contribute to the efficient and fast separation of lipase from the reaction mixture under external magnetic fields, and thus facilitate the economical and practical applications of lipase in hydrolysis, esterification and transesterification in chemical, pharmaceutical and food industries.

Experimental

Materials. Ferrous chloride tetrahydrate ($FeCl_2{\cdot}4H_2O$),

ferric chloride hexahydrate ($FeCl_3 \cdot 6H_2O$) were obtained from Sigma Chemical Co. (St. Louis, MO, USA). Tetraethyl orthosilicate (TEOS), (3-aminopropyl) triethoxysilane (APTES) and ammonium hydroxide (25%, w/w) were purchased from Aladdin (Shanghai, China). Lipase (Produced from Bohaisea-9145) was self-cultivated and purified. All chemicals were of analytical grade and used without further purification.

Synthesis of Monodisperse Fe_3O_4 NPs. $FeCl_2 \cdot 4H_2O$ (4.0 g) and $FeCl_3 \cdot 6H_2O$ (10.8 g) were dissolved in 100 mL distilled water under under argon protection. Ammonia water (50.0 mL, 28%-30%) was added into the solution drop by drop until the pH reaches 9.0. After being stirred for 20 min, the reaction temperature was increased to 80 °C and sustained for 2 h. The obtained black precipitate was separated by magnetic decantation and was washed several times with distilled water and ethanol. The magnetic nanoparticles were dried under reduced pressure.

Synthesis of Fe_3O_4@SiO_2 NPs (denoted as Fe_3O_4@SiO_2). The silica shell onto particles was synthesized *via* hydrolysis of TEOS in basic solution *via* Stöber's method with minor modification. Briefly, 100 mg magnetite nanoparticles were dispersed into a mixture of 80 mL ethanol and 20 mL distilled water in argon atmosphere and sonicated for 15 min, followed by the addition of 2.5 mL ammonia water. 2 mL tetraethyl orthosilicate (TEOS) was then added to the reaction solution under vigorous stirring. The resulting dispersion was mechanically stirred for 4 h at room temperature. The magnetic Fe_3O_4@SiO_2 nanoparticles were collected by magnetic separation and washed with ethanol and deionized water, and dried under reduced pressure.

Aminopropyl Modified Fe_3O_4@SiO_2 NPs (denoted as Fe_3O_4@SiO_2-NH_2). Briefly, 10 mg Fe_3O_4@SiO_2 NPs were dispersed into 50 mL toluene and sonicated for 10 min, followed by the addition of 2.0 mL ammonia. 200 μL (3-aminopropyl) triethoxysilane (APTES) was then added into the above solution under vigorous stirring in argon atmosphere. The final product was magnetically separated, completely washed with toluene. This coating formed an extra NH_2-silica layer.

Lipase Immobilization onto Fe_3O_4@SiO_2-NH_2. 10 mg Fe_3O_4@SiO_2-NH_2 NPs was added to phosphate buffere (pH 8.0, 50 mM) containing different amounts of lipase. The mixture was stirred at 200 rpm and 30 °C for 10 h. The immobilized protein was separated by magnetic decantation of the supernatant. The resulting immobilized lipase was washed using the same buffer until no protein could be detected. The amount of adsorbed protein on the supports was determined by measuring the protein concentration of the lipase solution and the supernatant by the Bradford method[28].

Enzyme Activity Assay. Activity of the free or immobilized lipase was assayed using *p*-NitroPhenyl-Laurate (pNPL) as substrate. The assay procedure followed a reported literature[29] with minor modification. Briefly: Solution A: 40 mg of pNPL was dissolved in 12 mL isopropanol. Solution B: 0.4 g Triton X-100 was dissolved in 90 mL of 100 mM potassium phosphate buffer pH 7.0. The substrate solutions were prepared by dropwise addition of 0.2 mL solution A (pNPL) into 3 mL solution B under intense vortexing, which were stable for 1 h at room temperature.

To check the activity of the free lipase or immobilized lipase, a mixture of 0.1 mL A and 1.5 mL B was incubated at 35 °C for 3 min. Certain amount of free lipase or immobilized lipase were then added and incubated for 8 min. The reaction was terminated by boiling for 5 min, followed by centrifuging at 5000 rpm for 10 min (magnetic adsorption in the case of immobilized lipase). The amount of the product was checked by measuring absorbance of the supernatant at 410 nm. A boiled (5 min) enzyme sample undergone the same treatment, was used as a blank. One unit (U) of enzyme activity was defined as the amount of enzyme required for the liberation of 1 μmol pNP per minute under the assay conditions. The extinction coefficient of the pNP anion was 16 $mM^{-1}.cm^{-1}$.[29]

Characterizations

The bare and composite Fe_3O_4 MNPs were characterized respectively by FT-IR analysis, X-ray diffraction analysis, TEM, magnetic measurements, and TGA. The IR spectra were recorded in the range 4000 to 400 cm^{-1} using KBr pellets on a Bruker Tensor 27 FT-IR spectrometer. The powder X-ray diffraction scans of samples were carried out on a Bruker D8 Advance Diffractometer using Cu-Kα radiation (40 kV, 40 mA). Diffractograms were obtained using continuous scanning mode from 5° (2θ) to 80° (2θ) at a rate of 4° min^{-1}. The TEM images were recorded by a JEOL JEM-1200EX transmission electron microscope. The samples for TEM studies were suspended in ethanol in order to disperse the powders and a drop of the sample was deposited on a lacey carbon copper grid as a TEM support. The grid was dried under reduced pressure for 2 h at room temperature. The accelerating voltage of the TEM was 200 kV. The magnetic properties were performed at 300 K using a Quantum Design MPMS-XL 7 magnetometer. The TGA was carried out on a Netzsch STA409PC instrument in N_2 atmosphere (flow rate = 60 mL min^{-1}) at a heating rate of 10 ºC min^{-1} from 20 to 974 ºC.

Results and Discussion

FT-IR Analysis. Figure 1 shows the FT-IR spectra of the nanoparticles. The characteristic absorption of bare Fe_3O_4 (curve a) was observed at 579 cm^{-1} (Fe-O vibrations). The spectrum of Fe_3O_4@SiO_2 NPs (curve b) showed strong peaks at 1083 cm^{-1} and 799 cm^{-1}, respectively, which could be assigned to the un-symmetric and symmetric linear stretching vibrations of Si-O-Si bonding. The bending vibration absorption peaks of Si-O-Si and Si-OH were observed at 461 cm^{-1} and 962 cm^{-1} respectively. These indicated the existence of silica layer on SMNP. In the spectrum of Fe_3O_4@ SiO_2-NH_2 (curve c), the two bands at 3422 cm^{-1} and 1644 cm^{-1} can be referred to the N-H stretching vibration and NH_2 bending mode of free NH_2 group, respectively. The anti-

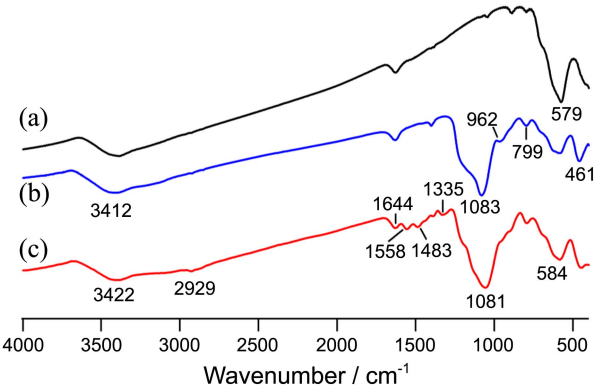

Figure 1. IR spectra of bare Fe_3O_4 (a), Fe_3O_4@SiO_2 (b) and Fe_3O_4@ SiO_2-NH_2 NPs (c).

symmetric and symmetric C-H stretching vibrations appeared at 2929 cm^{-1} and 2857 cm^{-1}, respectively, and the bending vibration absorption peaks of -CH_2 and -CH_3 appeared in 1489 cm^{-1} and 1388 cm^{-1}, respectively; The C-N stretching vibrations appeared at 1335 cm^{-1}. The deformation vibration absorption peak of N-H appeared at 1558 cm^{-1}. These indicated the successful introduction of APTES to the surface of magnetic NPs.

TEM. The TEM images of three types of nanoparticles are shown in Figure 2. The TEM observation indicates that the obtained Fe_3O_4 nanoparticles have diameters around 7.6 nm (Fig. 2(a)), and it demonstrated spherical morphology. As shown in Figure 2(b), the size of the MNPs slightly increased to 8 nm after the modification of Fe_3O_4 NPs using TEOS. A amino layer was further coated on the surface of the synthesized Fe_3O_4@SiO_2 NPs, producing Fe_3O_4@SiO_2-NH_2 NPs with an average size of 10 nm as shown in Figure 2(c).

XRD Analysis. The X-ray diffraction patterns of bare Fe_3O_4, Fe_3O_4@SiO_2 and Fe_3O_4@SiO_2-NH_2 NPs were shown in Figure 3(a)-(c), respectively. The characteristic peaks in the spectrum of Fe_3O_4 (Fig. 3(a)) agree well with the standard Fe_3O_4 (cubic phase) XRD spectrum. The peaks at 2θ = 30.2°, 35.6°, 43.2°, 57.3° and 62.9° were assigned to (220), (311), (400), (422), (511) and (440) reflections,[30] respectively. The above peaks were also observed in the spectrum of Fe_3O_4@SiO_2 NPs (Fig. 3(b)) and Fe_3O_4@SiO_2-NH_2 NPs (Fig. 3(c)) except for the peak existed at 2θ = 25°, which

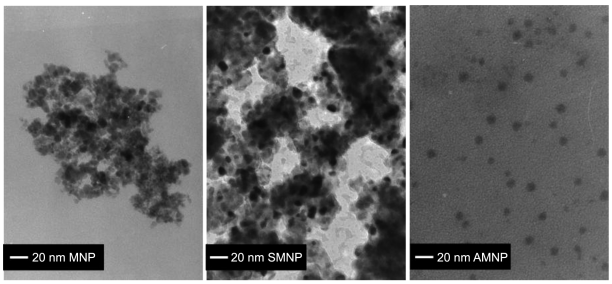

(a) Fe_3O_4 (b) Fe_3O_4@SiO_2 (c) Fe_3O_4@SiO_2-NH_2

Figure 2. TEM images of Fe_3O_4 (a), TEOS (b) and APTES (c) modified nanoparticles.

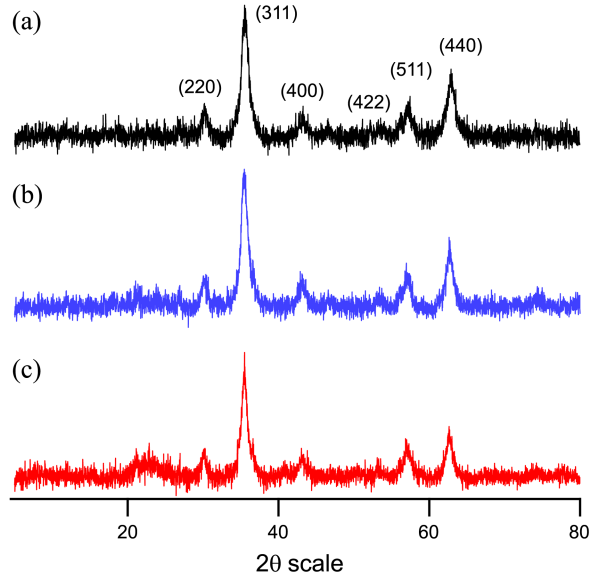

Figure 3. XRD patterns of bare Fe_3O_4 (a) Fe_3O_4@ SiO_2 (b) and Fe_3O_4@SiO_2-NH_2 (c) nanoparticles.

might be attributed to the existence of amorphous SiO_2. This illustrated that the crystalline structure of the modified nanoparticles was not changed during the modification process, indicating the surface modification and conjugation of the Fe_3O_4 nanoparticles didn't affect the physical properties of the magnetite particles. The broadening of each peak in XRD mean crystallite size was calculated by applying Scherrer's equation: $D = K\lambda/\beta\cos\theta$, where D is the average diameter, *K* is Sherrer constant, λ is ray wavelength (0.15406 nm), β is the peak width of half-maximum, and θ is the Bragg diffraction angle. The mean crystallite size for bare Fe_3O_4 NPs was found to be 7.6 nm, which is basically in accordance with the TEM result.

Magnetic Properties. In order to study their magnetic behavior, the magnetic properties of the magnetic NPs were measured at room temperature using VSM. The hysteresis loops of the samples are shown in Figure 4. The saturation magnetizations for bare Fe_3O_4, Fe_3O_4@SiO_2 and Fe_3O_4@SiO_2-NH_2 NPs were found to be 48 emu/g, 33 emu/g and 20 emu/g, respectively. The saturation magnetization decreased during the function modification process, indicating the coating

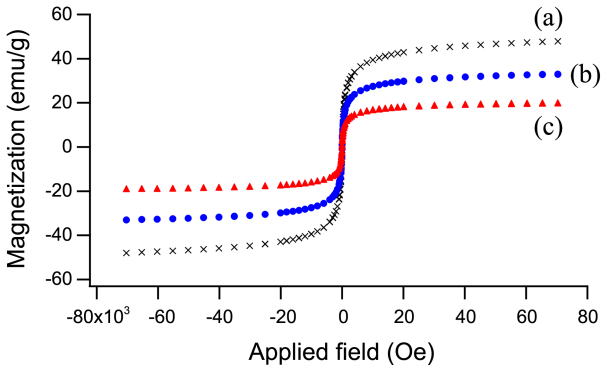

Figure 4. Hysteresis loop of Fe_3O_4 (a), Fe_3O_4@SiO_2 (b), and Fe_3O_4@SiO_2-NH_2 (c) nanoparticles.

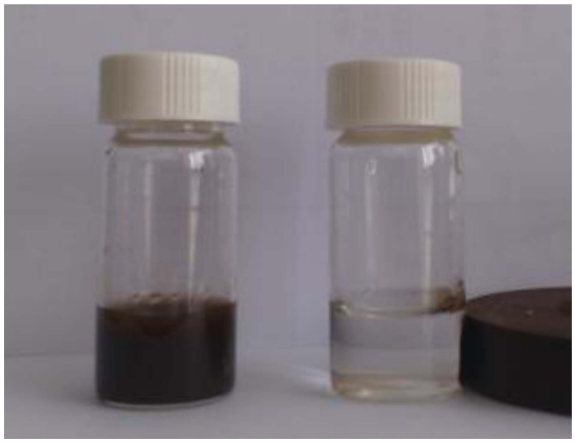

Figure 5. Photographs of aqueous suspension of Fe_3O_4 and its modified nanoparticles before (a) and after (b) magnetic capture.

formation on the surface of the MPs probably affects the magnetic ability. All of these three NPs showed negligible coercivity (Hc) and remanence, typical of superparamagnetic materials.

To further investigate the performace of Fe_3O_4@SiO_2-NH_2 NPs under magnetic enviroment, Fe_3O_4@SiO_2-NH_2 NPs were dispersed in water, resulting in a dark black dispersion. Then a magnet was placed near the cuvette to separate the nanoparticles. Within about 2 min, the nanoparticles were completely aggregated to the cuvette wall and the dispersion became clear and transparent (Fig. 5). These good magnetic properties suggest that the prepared nanoparticles can potentially be used for magnetic field-guided targeting.

TGA. The thermal stability of the Fe_3O_4, Fe_3O_4@SiO_2 and Fe_3O_4@SiO_2-NH_2 NPs was evaluated by TGA. As shown in Figure 6, Fe_3O_4 NPs showed good thermal stability, and no apparent weight loss was observed (curve a). In the case of Fe_3O_4@SiO_2 NPs (curve b), 2.6% weight loss between 20 °C and 150 °C is due to loss of physically adsorbed water molecules on the surface. The weight loss 10.4% between 150 °C and 970 °C is presumably due to the loss of free water and bound water in SiO_2 Layer. The weight loss of APTES-modified magnetic NPs between 150 °C and 970 °C

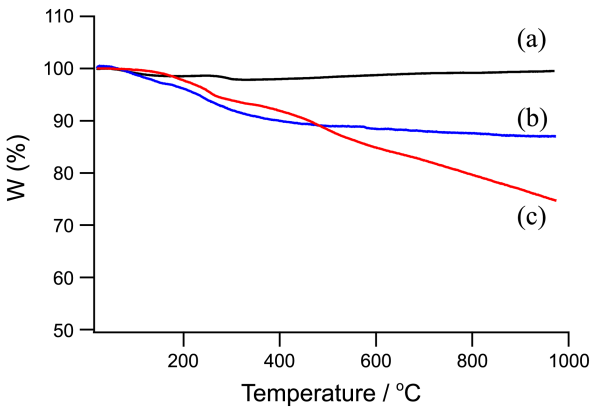

Figure 6. Weight loss analysis from TG curves of (a) Fe_3O_4, (b) Fe_3O_4@ SiO_2 and (c) Fe_3O_4@SiO_2-NH_2 nanoparticles.

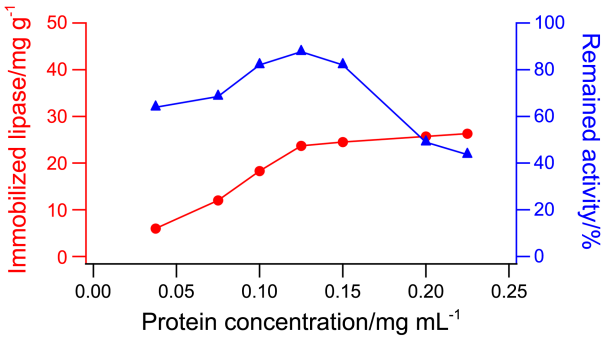

Figure 7. Amounts of Fe_3O_4@SiO_2-NH_2 immobilized lipase and the remained activity.

was about 31.8%, indicating the APTES coating contributed about 20% weight loss to the MPs (curve c).

Immobilization of Lipase onto Fe_3O_4@SiO_2-NH_2. Lipase could be immobilized onto the Fe_3O_4@SiO_2-NH_2 NPs (Fig. 7). The amount of protein adsorbed onto the supports increased with the increase of the protein concentration during the range of 0.0375 to 0.225 mg mL^{-1}, and the maximum absorption was achieved to 26.3 mg g^{-1}, while the protein concentration was 0.225 mg mL^{-1}.

The remained activity of the immobilized lipase firstly increased with the increase of the amounts of immobilized protein, and the maximum activity was achieved (88%) while the amount of immobilized lipase was 23.7 mg g^{-1}. The remained activity decreased while the amount of immobilized protein further increased, indicating too much protein on the surface affected the catalytic ability.

Conclusions

To develop magnetic nanoparticles for protein immobilization, monodisperse Fe_3O_4 NPs were initially synthesized using coprecipiation method. A layer of SiO_2 was coated on the Fe_3O_4 NPs by using a modified Stöber's method to avoid aggregation of the Fe_3O_4 NPs. The magnetic nanoparticles were easily coated with silica shell as the iron oxide surface has a strong affinity for silica. To further improve the dispersity and biocompatibility, APTES was utilized for the further modification, resulting in the formation of Fe_3O_4@ SiO_2-NH_2 particles with a diameter of about 10 nm. The as-synthesized Fe_3O_4@SiO_2-NH_2 NPs showed good magnetic propeties, which could imobilize lipase with a maximum absorption of 26.3 mg g^{-1}. The maximum maintained activity (88 percent) was achieved while the amount of immobilized lipase was 23.7 mg g^{-1}. The as-synthesized Fe_3O_4@SiO_2-NH_2 NPs not only have a wide promise to protein immobilization but also allow the efficient and fast separation from the reaction mixture in the presence of external magnetic field. Therefore, the utilization of as-synthesized Fe_3O_4@ SiO_2-NH_2 NPs in protein immobilization would facilitate their economical and practical applications of lipase in industry. Furthermore, Fe_3O_4@SiO_2-NH_2 NPs can potentially be used for magnetic field-guided targeting.

Acknowledgments. We thank the support of this work by NSFC (No. 31200642), National High Technology Research and Development Program of China (No. 2011AA090703), The international scientific and technological cooperation projects of China (No. 2011DFB30250), Special Scientific Research Funds for Central Non-profit Institutes, Chinese Academy of Fishery Sciences (No. 2013A1002), and Qingdao Municipal Science and Technology Plan Project (No. 12-1-4-12-(2)-jch). And the publication cost of this paper was supported by the Korean Chemical Society.

References

1. Jang, J. H.; Lim, H. B. *Microchem. J.* **2010**, *94*, 148.
2. Dios, A. S.; Diaz-Garcia, M. E. *Anal. Chim. Acta* **2010**, *666*, 1.
3. Park, H. J.; McConnell, J. T.; Boddohi, S.; Kipper, M. J.; Johnson, P. A. *Colloids Surf., B* **2011**, *83*, 198.
4. Gong, J. L.; Liang, Y.; Huang, Y.; Chem, J. W.; Jiang, J. H.; Shen, G. L.; Yu, R. Q. *Biosens. Bioelectron.* **2007**, *22*, 1501.
5. Qi, H.; Li, S. Q.; Liang, L.; Ling, C.; Gao, Q.; Zhang, C. *Spectrochim. Acta, Part A* **2011**, *82*, 498.
6. Sung, Y. J.; Suk, H. J.; Sung, H. Y.; Li, T.; Poo, H.; Kim, M. G. *Biosens. Bioelectron.* **2013**, *43*, 432.
7. Xuan, J.; Jia, X. D.; Jiang, L. P.; Abdel-Halim, E. S.; Zhu, J. J. *Bioelectrochemistry* **2012**, *84*, 32.
8. Li, J.; Zhou, Y.; Li, M.; Xia, N.; Huang, Q. Y.; Do, H.; Liu, Y. N.; Zhou, F. M. *J. Nanosci. Nanotechno.* **2011**, *11*, 10187.
9. Sayin, S.; Ozcan, F.; Yilmaz, M. *Mater. Sci. Eng., C* **2013**, *33*, 2433.
10. Klostergaard, J.; Seeney, C. E. *Maturitas*. **2012**, *73*, 33.
11. Hua, M. Y.; Liu, H. L.; Yang, H. W.; Chen, P. Y.; Tsai, R. Y.; Huang, C. Y.; Tseng, I. C.; Lyu, L. A.; Ma, C. C.; Tang, H. J.; Yen, T. C.; Wei, K. C. *Biomaterials* **2011**, *32*, 516.
12. Mahapatra, A.; Mishra, B. G.; Hota, G. *Ceram. Int.* **2013**, *39*, 5443.
13. Girginova, S.; Daniel-da-Silva, A. L.; Lopes, C. B.; Figueira, P.; Otero, M.; Amaral, V. S.; Pereira, E.; Trindade, T. *J. Colloid Interface Sci.* **2010**, *345*, 234.
14. Anirudhan, T. S.; Rauf, T. A. *Colloids Surf., B* **2013**, *107*, 1.
15. Tran, D. T.; Chen, C. L.; Chang, J. S. J. *Biotechnol.* **2012**, *158*, 112.
16. Jiang, Y. Y.; Guo, C.; Xia, H. S.; Mahmood, I.; Liu, C. Z.; Liu, H. Z. *J. Mol. Catal. B: Enzym.* **2009**, *58*, 103.
17. Liao, H. D.; Chen, D.; Yuan, L.; Zheng, M.; Zhu, Y. H.; Liu, X. M. *Carbohydr. Polym.* **2010**, *82*, 600.
18. Gokhale, A. A.; Lu, J.; Lee, I. *J. Mol. Catal. B: Enzym.* **2013**, *90*, 76.
19. Mahmood, I.; Ahmad, I.; Chen, G.; Liu, H. Z. *Biochem. Eng. J.* **2013**, *73*, 72.
20. Liang, H. F.; Wang, Z. C. *Mater. Chem. Phys.* **2010**, *124*, 964.
21. Liu, X.; Lei, L.; Li, Y. F.; Zhu, H.; Cui, Y. J.; Hu, H. Y. *Biochem. Eng. J.* **2011**, *56*, 142.
22. Li, Z. L.; Wang, Y. J.; Sheng, J.; Liu, J. Z.; Sun, M. *Oceanologia Et Limnologia Sinica* **2012**, *43*, 230.
23. Shao, T. J.; Sun, M.; Zheng, J. S.; Wang, Y. J.; Qiu, X. B. *Acta Microbiologica Sinica* **2004**, *44*, 789.
24. Dong, H. W.; Sun, M.; Wang, Y. J.; Yu, J. S. *Oceanologia Et Limnologia Sinica* **2004**, *35*, 376.
25. Schultz, N.; Syldatk, C.; Franzreb, M.; Hobley, T. J. *J. Biotechnol.* **2007**, *132*, 202.
26. Kuo, C. H.; Liu, Y. C.; J. Chang, C. M.; Chen, J. H.; Chang, C.; Shieh, C. J. *Carbohydr. Polym.* **2012**, *87*, 2538.
27. Cui, Y. J.; Li, Y. F.; Yang, Y.; Liu, X.; Lei, L.; Zhou, L.; Pan, F. *J. Biotechnol.* **2010**, *150*, 171.
28. Bradford, M. M. *Anal. Biochem.* **1976**, *72*, 248.
29. Hatzinikolaou, D. G.; Kourentzi, E.; Stamatis, H.; Christakopoulos, P.; Kolisis, F. N.; Kekos, D.; Macris, B. J. *J. Biosci Bioeng.* **1999**, *88*, 53.
30. Park, J. O.; Rhee, K. Y.; Park, S. J. *Appl. Surf. Sci.* **2010**, *256*, 6945.